

Study on Electrical, Thermal, Magnetic Properties and Microstructure for α -Al, θ -Al₂Cu, ω -Al₇Cu₂Fe Phases in Al-32.5 wt. % Cu-1 wt. % Fe Ternary Alloy

Canan Alper Billur ^{1,a,*}, Buket Saatçi ^{2,b}¹ Sivas Vocational School of Technical Sciences, Sivas Cumhuriyet University, Sivas, Türkiye.² Department of Physics, Erciyes University, Kayseri, Türkiye.

*Corresponding author

Research Article

History

Received: 24/08/2023

Accepted: 24/11/2023







This article is licensed under a Creative Commons Attribution-NonCommercial 4.0 International License (CC BY-NC 4.0)

ABSTRACT

The electrical properties of the Al-32.5 wt. % Cu-1 wt. % Fe ternary alloy were examined, it was observed that the electrical resistivity increased depending on the temperature and it was found as $6.8546 \times 10^{-8} \Omega \cdot m - 5.7780 \times 10^{-7} \Omega \cdot m$ in the temperature range of 298-810K. The thermal conductivity was calculated using electrical measurement results and it was observed that it decreased depending on the temperature. The ternary alloy (cubic α -Al, Fm-3m, 225 a = 4.0480 Å, θ -tetragonal Al₂Cu, I4mcm, 140, a=6.0654 Å c=4.8732 Å, ω -tetragonal Al₇Cu₂Fe, P4 /mnc, 128, a = 6.3360 Å, m and c = 14.87 Å) phases were obtained. In this ternary alloy, phases were clearly seen in XRD studies and EDAX analyzes at room temperature. Magnetic properties such as magnetic transition temperature and magnetization curves of the alloy were determined.

Keywords: Mechanical properties, Electrical properties, Thermal properties, Magnetic properties, Intermetallic phase.

 cbillur@cumhuriyet.edu.tr <https://orcid.org/0000-0002-6888-8013> bayender@erciyes.edu.tr <https://orcid.org/0000-0002-1351-5279>

Introduction

The discovery of quasicrystals (QCs) has been one of the most intense investigations in recent decades in terms of the investigation of its structure and the determination of its properties. Studies on many systems under stable or metastable conditions were defined as QC forms. Most of these systems are based on aluminum alloying with transition metals. Although a lot of scientific knowledge about QCs has already emerged, the technological use of these materials has not yet been reached. Its use as a reinforcement phase in aluminum alloys is promising [1]. Aluminum alloys are widely used in the automotive and aerospace industries due to their light weight and satisfactory mechanical properties [2]. Al-Cu-Fe alloys, which are aluminum alloys, are typical materials in which semi-crystals appear. These alloys are interesting because of their non-toxicity, easy availability, and affordable cost of alloying elements [3] and interest in Al-Cu-Fe quasicrystals, the fact that they have an unusual combination of physics micromechanical properties [4]. Tsai *et al.* first reported a stable icosahedral quasicrystal forming composition [5]. Again, the mechanical properties of the Al-Cu-Fe ternary metallic alloy were obtained by Tsai *et al.* with the Vickers test. It has a composition around Al₆₅Cu₂₀Fe₁₅ in the Al-Cu-Fe ternary system. Besides, the equilibrium phase diagram of the Al-rich Al-Cu-Fe alloy system has been the subject of several previous studies [6–12].

Also recently, laser processing of Al-Cu-Fe alloys has become an attractive process to obtain high-quality coatings [13,14]. The change in electrical and magnetic properties of Al-Cu-Fe semi-crystals (QCs) has also been studied recently. The structure of icosahedral Al-Cu-Fe shows ferromagnetic properties. Al-Cu-Fe QCs powder was studied in detail using a vibrating sample magnetometer (VSM) [15].

In the Al-Cu-Fe system, the icosahedral quasicrystalline is stable in a certain composition range when the ψ phase is in equilibrium with the β -AlFe(Cu), λ -Al₁₃Fe₄, λ 1-Al₃ Fe, θ -Al₂ Cu, ω -Al₇Cu₂ Fe and ϕ -Al₁₀Cu₁₀Fe phases [3]. The coordination of Fe atoms in the ω phase is very similar to the icosahedral (Al₆₃Cu₂₅Fe₁₂ (at. %)) ψ phase [16].

In this study, θ -Al₂Cu, ω -Al₇Cu₂Fe intermetallic phases formed by adding Cu element to Al-Cu binary eutectic alloy were observed and mechanical, electrical, thermal and magnetic properties of the obtained ternary alloy were determined.

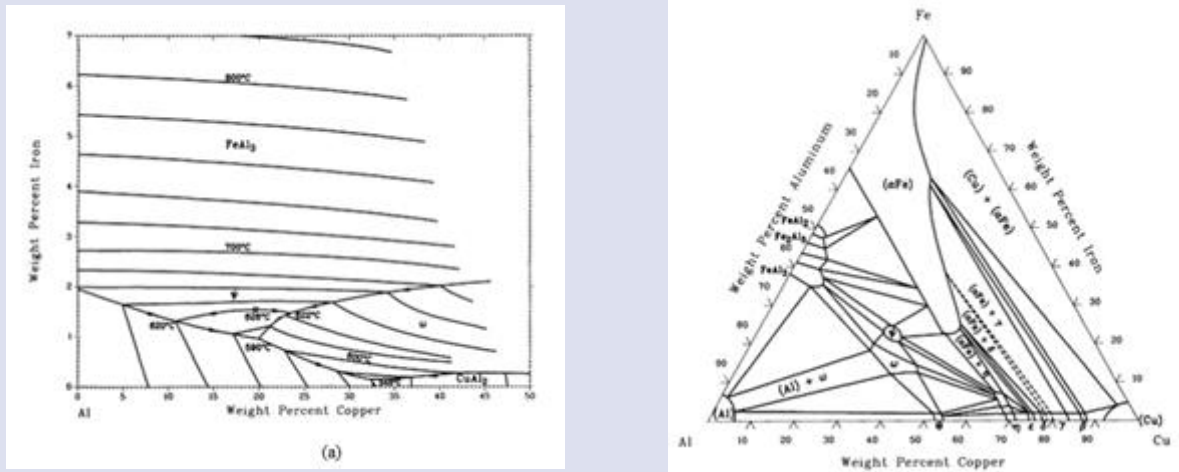


Figure 1. Al-Cu-Fe Ternary Phase diagram. Al-Cu binary, b) Al-Cu-Fe Ternary [17,18].

Experimental Method

The Al-32.5 wt. % Cu-1 wt. % 1 Fe sample was determined from the relevant phase diagram related to stoichiometric calculations as seen in Figure 1 [17-18]. After weighing the masses of the Al, Cu, Fe elements (Alfa Aesar, 4N in purity) whose composition was determined from the phase diagram, they were placed in the graphite crucible in the vacuum melting furnace according to their melting temperatures. A homogeneous alloy was obtained from the elements melted without oxidation in the vacuum melting furnace. Then the homogenized alloy was cast in the hot casting furnace without any air bubbles into 5 cylindrical graphite molds which is 200 mm height, 4 mm inner diameter and outer diameter of 6.35 mm. The samples obtained after the casting stage were cut and placed in the mold and then used for the desired purposes (for XRD, SEM, EDAX, mapping, DTA, electrical resistivity, magnetization) in this study.

Determination of the Electrical Resistivity

The conductivity and temperature resistance coefficient, which are important electrical properties of the material, determine the use of from wire to resistors, potentiometers and many more in electrical and electronic components. Electrons carry the current in metals without changing the chemical properties of metal. Electrical conductivity (EC), one of the physical properties of the material, is affected by the chemical composition of the substances and the stress of the crystal structure. For this reason, electrical conductivity is a parameter used for many purposes such as determining the appropriate heat treatment for metals, controlling heat damage in materials, as well as classifying materials.

Standard conversion method [19,20] was used in the measurement of electrical resistance and conductivity. The temperature dependence of the electrical resistivity of the sample was determined using standard DC four-point probe method (FPPM) in the temperature range of 298-810K (Figure 2). In the DC FPPM, measurement errors have been blocked due to probe resistance, spread resistance under each probe, and contact resistances between metal probes and material [21].

Electrical measurement of the sample was taken on samples with 4 mm diameter. A Keithley 2400 SourceMeter was used to provide constant current, and potential drop was measured by a Keithley 2700 Multimeter through an interface card, which was controlled by a computer in previous study. While using the known conversion rule between electrical resistivity and conductivity, voltage drop is determined by using platinum wires with 0.5 mm radius as current and potential probes [19,22]. At the same time, the electrical resistance temperature coefficient was calculated using the electrical resistance results in the temperature range of 298-810 K [21].

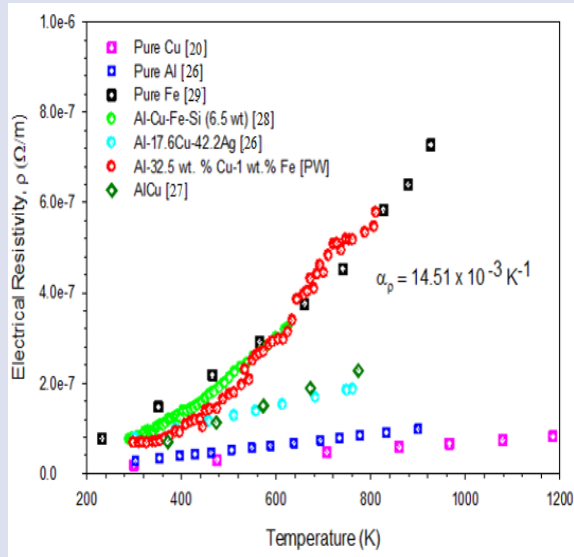


Figure 2. The graph of variation of electrical resistivity with temperature.

Calculation of Thermal Conductivity

Along with electrons, phonons also contribute to thermal conductivity. The relation between thermal conductivity and electrical resistivity is explained by the Wiedemann-Franz-Lorenz law [23].

$$\frac{\kappa}{\sigma T} = \frac{\pi^2 k^2}{3e^2} = L_0 = 2.445 \times 10^{-8} W\Omega K^{-2} \quad (1)$$

where $\kappa, \sigma, T, k, e, L_0$ represent thermal conductivity, electrical conductivity, temperature, Boltzmann constant, electron charge, Lorenz number, respectively. The electrical conductivity and the thermal conductivity can be connected via the W-F law as follows:

$$\sigma = \frac{\kappa_s}{LT} \quad (2)$$

where σ is the electrical conductivity, κ_s is the thermal conductivity, T is temperature, and L is the Lorenz number.

In this study, thermal conductivity values for Al-32.5 wt. % Cu – 1 wt. % Fe composition of alloy was calculated from W-F equation using electrical measurement results. While the value of L is well known for pure materials, it is not well known for alloys as it depends on the property of the material. L and κ_s are required to show electrical resistivity change with temperature and composition. The Lorenz numbers for pure Al, Cu and Fe are $2.24 \times 10^{-8}, 2.49 \times 10^{-8}$ and $2.55 \times 10^{-8} W\Omega/K^2$ [24].

$$L_{alloy} = \sum_{n=1}^2 x_n L_n \quad (3)$$

Lorenz value for Al-Cu-Fe ternary alloy was calculated from Eq. (3). x_n is the percent by weight of the n^{th} component; L_n is the percent of the Lorenz value of the n^{th} component.

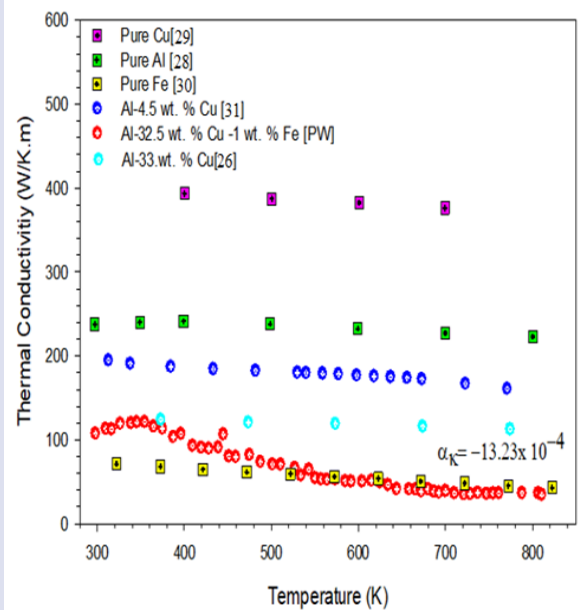


Figure 3. The graph of variation of thermal conductivity with temperature

Characterization Studies

The crystal structure analysis was carried out at room temperature using the Panalytical Empyrean Model Diffractometer. The XRD patterns of the produced samples were obtained using Cu-K α radiation at a wavelength of 1.54 Å and a scanning step of 0.02 °/sec from 10° to 90°. The X-rays scattered from distinct atomic planes were detected by the thallium-activated sodium iodide detector (NaI) scintillation counter. The Win-Index and X-Powder software programs were employed for evaluating the XRD patterns and calculating crystal structure parameters, such as crystal size. The Perkin Elmer Diamond TG & DTA device was utilized for investigating temperature-dependent thermal events such as transitions in phase and weight loss.

This system's heating rate was set at 10 °C/min in order to precisely observe endothermic or exothermic peaks on the DTA curves, suggesting a possible phase transition. The morphological features of materials were studied using Field-Emission Scanning Electron Microscopy (FE-SEM) technique by the ZEISS Gemini SEM 500 model device

Also, DTA and TGA measurements were made depending on the temperature of Al-32.5 wt. % Cu – 1 wt. % Fe alloy. During uniform heating, a shape endothermic peak is present in the DTA curves, indicating a possible phase transition. The endothermic reactions show heat entering the sample, and exothermic reactions show heat leaving the sample during the heating or cooling process [25].

After electrical measurements, XRD and DTA and TGA analysis were performed on the sample obtained in the study, the microstructure of the sample was examined. While examining the microstructure of the samples, FE-SEM images were also taken, and EDAX and Mapping analyzes were performed with FE-SEM apparatus from the same region at the same time.

Magnetic Properties

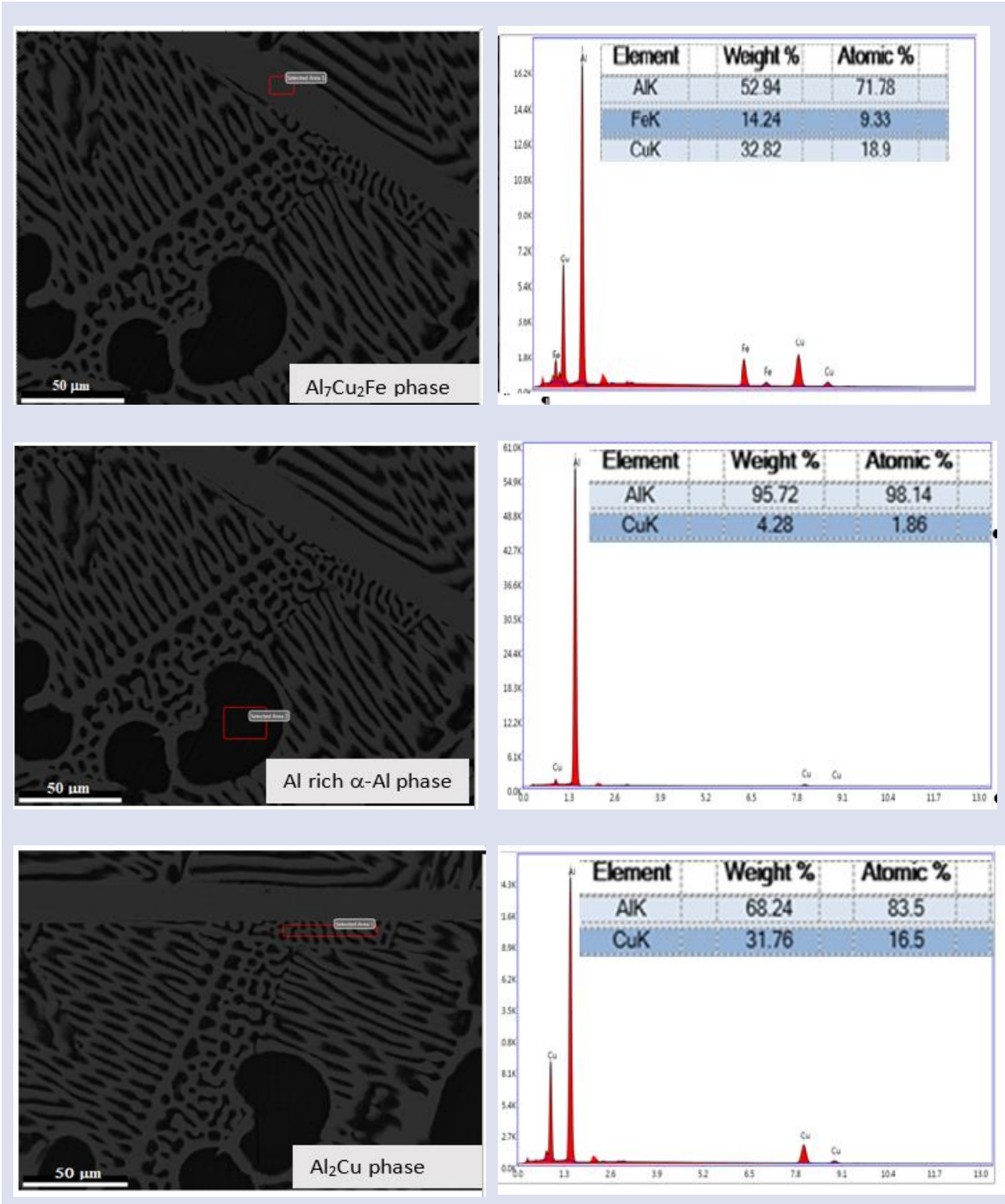
In this study, the magnetic property of the Al-Cu-Fe alloy was determined with a Quantum Design-PPMS DynaCool-9 model device, which can apply a magnetic field up to 9 T in the temperature range of 1.8-600 K. Magnetic field (M-H) and temperature-dependent magnetization (M-T) measurements were made with this device. The experimental magnetic transition temperatures (T_c) were determined by the first derivative of the magnetization curves.

Results and Discussion

Electrical resistivity of Al-Cu-Fe alloy was measured by FPPM method depending on temperature. In the measurements obtained at 298-810 K in temperature range, it was found that the resistance increased linearly with temperature.

Table 1. The elemental composition of Al-32.5 wt. % Cu-1 wt. % Fe, α -Al, θ -Al₂Cu ω -Al₇Cu₂Fe phases as determined by EDAX.

Phase	Al (at. %)	Al(wt. %)	Cu (at. %)	Cu(wt. %)	Fe (at. %)	Fe (wt. %)
α -Al	98.14	95.72	1.89	4.28
θ -Al ₂ Cu	83.5	68.24	16.5	31.76
ω -Al ₇ Cu ₂ Fe	71.78	52.94	18.19	32.82	9.33	14.24



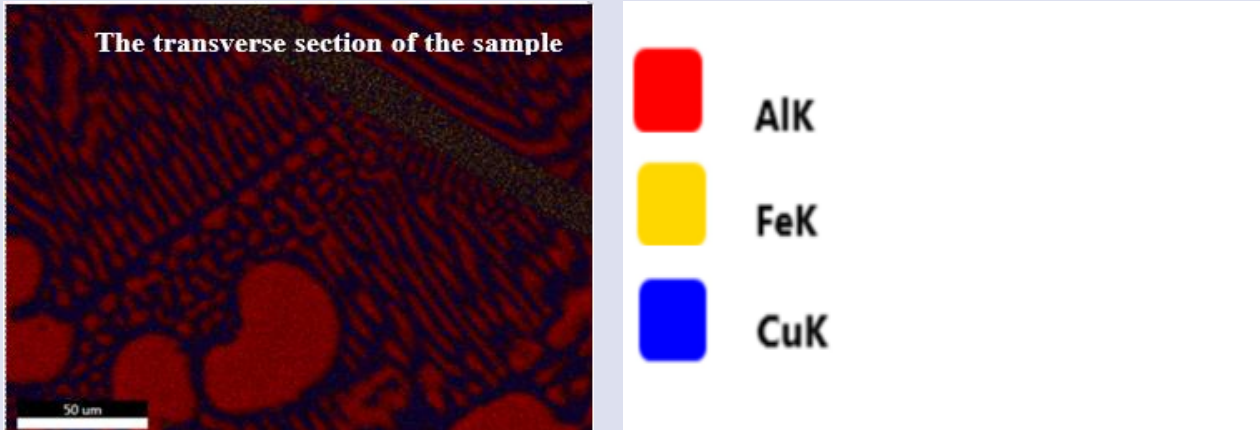


Figure 4. FE-SEM and MAPPING images of the Al-32.5 wt. % Cu- 1 wt. % Fe sample.

Increasing the temperature of the alloy will decrease the mean free path. This is due to lattice vibrations that increase with temperature. With the decrease of the mean free path, the electrical conductivity will decrease while the electrical resistivity will increase. At the same time, alloys have higher electrical resistivity than pure metals. When the electrical resistivity values of the alloy were compared with the literature results, it was determined that the electrical resistivity of the Al-Cu-Fe alloy was higher than the pure Al[26] and Cu[20], Al-Cu[27] alloy, Al-Cu-Ag[26] alloy. When compared with pure Fe[29], the amount of Fe in our Al-Cu-Fe alloy increased the electrical resistivity.

coefficient of the electrical resistance (TCR), α_p value of the alloy in the temperature range of 298-810 K was found to be $14.51 \times 10^{-3} \text{ K}^{-1}$ by using the electrical resistivity values [Figure 2].

Thermal conductivity values were calculated using W-F equation using electrical measurements results. It has been observed that the thermal conductivity values decrease depending on the temperature. This is expected because as the temperature increases, carrier electrons, holes and lattice vibrations increase. This combined situation may cause a decrease in electrical conductivity in some alloys and an increase in others. In our study, phonon-phonon and electron-phonon scattering became more prominent with the increase in lattice vibrations. This reduces the thermal conductivity. When the results were compared with the literature in Figure 3, it was seen that it was compatible with pure Al, Cu, Fe and other alloys.

The thermal conductivity value of the alloy in the temperature range of 298-810K was obtained between 107.4445 W/Km - 34.6622 W/Km. The temperature coefficient of the thermal resistance (TCTR), α_k value of the alloy in the temperature range of 298-810 K was found to be $14.51 \times 10^{-3} \text{ K}^{-1}$ by using the electrical resistivity values [Figure 3].

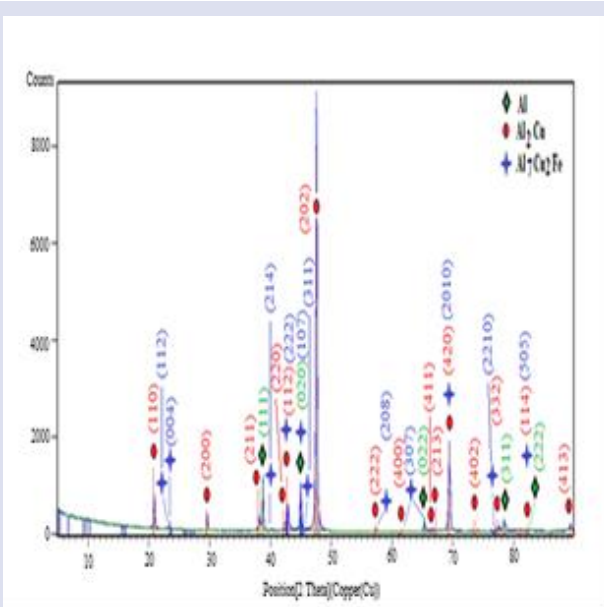


Figure 5. The graph of variation of thermal conductivity with temperature

The electrical resistivity value of the alloy in the temperature range of 298-810 K was obtained between $6.8546 \times 10^{-8} \text{ } \Omega\text{m}$ and $5.7780 \times 10^{-7} \text{ } \Omega\text{m}$. The temperature

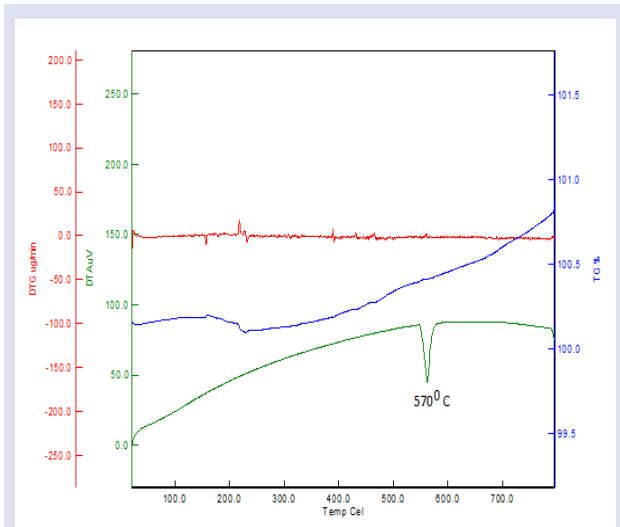


Figure 6. Thermal curves depending on temperature in the Al-32.5 wt. % Cu – 1 wt. % Fe ternary metallic alloy system.

were determined by microstructure analysis. The existence of these phases was confirmed by the phase diagram of the Al-Cu-Fe ternary alloy.

The microstructure of the alloy was visualized by FE-SEM [Figure 4]. It has been observed that the alloy has homogeneous and regular structure. No defects, gaps or cracks were observed. The phases imaged by SEM were determined by MAPPING. Cu and Fe elements in the alloy dissolved in the structure and took place as θ -Al₂Cu, ω -Al₇Cu₂Fe phases. At the same time, the α -Al phase was determined [Figure 4.]. The quantitative chemical composition of these phases determined by MAPPING are given by EDAX analysis [Table 1.]. With XRD diffraction peaks measurements, both phases were indexed and microstructure parameters such as crystal systems, space groups, cell parameters (a, b, c) of these phases were determined. When the indexed α -Al, θ -Al₂Cu, ω -Al₇Cu₂Fe phases were examined, it was observed that both the peak density and the peak intensity were in the Al₂Cu phase [Figure 5][Table 2.].

In the ternary alloy, multiple solid phases were formed simultaneously from the liquid phase and these phases

Table 2. In the study, the crystal system and cell parameters obtained in Al-Cu-Fe ternary metallic alloy.

Component of Ternary Alloy	Al							
	Space Group	Space group Number	Crystal System	Cell parameters			Volume of Cell (106 pm ³)	Crystallite Size only [Å]
				a(Å)	b(Å)	c(Å)		
Al-32.5 wt.% Cu-1 wt.% Fe	Fm-3m	225	Cubic	4.0406	4.0406	4.0406	65.97	39.8 ± 7.29
Component of Ternary Alloy	Al ₂ Cu							
	Space Group	Space group Number	Crystal System	Cell parameters			Volume of Cell (106 pm ³)	Crystallite Size only [Å]
				a(Å)	b(Å)	c(Å)		
Al-32.5 wt.% Cu-1 wt.% Fe	I4/mcm	140	Tetragonal	6.0654	6.0654	4.8732	179.28	39.00 ± 3.37
Component of Ternary Alloy	Al ₇ Cu ₂ Fe							
	Space Group	Space group Number	Crystal System	Cell parameters			Volume of Cell (106 pm ³)	Crystallite Size only [Å]
				a(Å)	b(Å)	c(Å)		
Al-32.5 wt.% Cu-1 wt.% Fe	P4mnc	128	Tetragonal	6.3360	6.3360	14.8700	596.65	47.00 ± 13.47

Also, Figure 6 show the DTA and TGA curves for sample Al-32.5 wt. % Cu – 1 wt. % Fe, as a function of temperature. In the observed endothermic reaction, the temperature was measured as 570 °C [Figure 6]

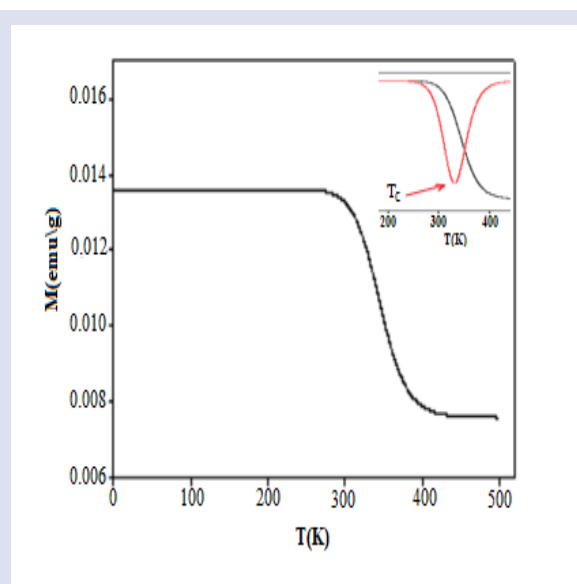


Figure 7. The temperature dependence magnetization curve of the two compositions Al-32.5 wt. % Cu- 1 wt. % Fe alloy. The inset present overlap $\partial M/\partial T$ curve as a function of temperature with M-T curve for determine to T_c

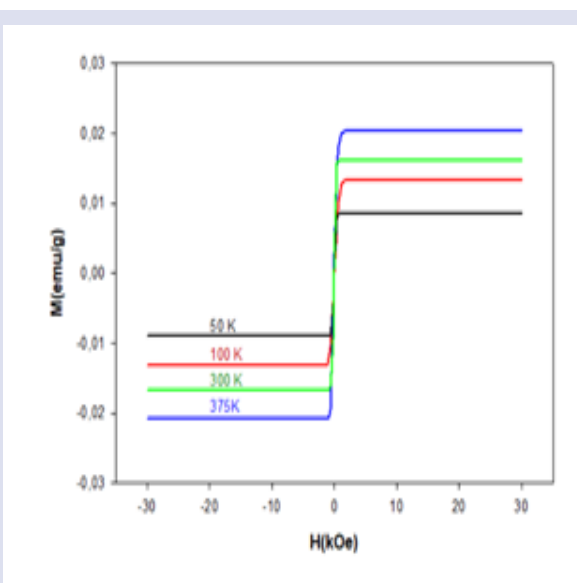


Figure 8. The magnetization as a function of applied field Al-32.5 wt. % Cu- 1 wt. % Fe alloy at 50 K, 100 K and 375 K degree temperature.

The temperature dependence of the magnetic field in the alloy was determined from the base temperature to the temperature of 500K in the 1kOe magnetic field. The Curie temperature, which is the magnetic transition temperature, was obtained from the Figure 7 graph, which gives the variation of the magnetic field with temperature. The Curie temperature (T_c) of the Al-32.5 wt. % Cu- 1 wt. % Fe alloy was found to be 343.4 K. We determined that the alloy exhibits ferromagnetic (FM)

properties from room temperature to the Curie temperature (T_c) and paramagnetic (PM) properties after T_c temperature (Figure 7). As can be seen from the magnetization hysteresis curve of the alloy in Figure 8, the magnetization curves decreased as the temperature increased. In the graph obtained for 50 K, 100 K, 300 K, 374 K temperature values, it was concluded that these were soft ferromagnetic materials with narrow hysteresis loops. For this reason, they exhibit a sigmoidal shape. Soft ferromagnetic materials have low remanence, low coercivity and low hysteresis loss. These results are compatible with the literature.[32-34].

Conclusion

Quasicrystals (QCs) which has icosahedral symmetry show the properties of heat and electrical conduction, high resistance and low expansion. In our study, an increase in electrical resistivity was observed with Fe added to the Al-Cu alloy. This supports the high resistance feature of quasicrystals (QC). At the same time, the decrease in thermal conductivity also supports heat conduction and, accordingly, expansion.

The results of the determined properties of the Al-32.5 wt. % Cu- 1 wt. % Fe alloy are given below

The electrical resistivity values increasing linearly with temperature were found in the $6.8546 \times 10^{-8} \Omega \text{m}$ - $5.7780 \times 10^{-7} \Omega \text{m}$ range.

The thermal conductivity values of the alloy calculated using the Wiedeman-Franz law are in the 107.4445 W/Km - 34.6622 W/Km range.

Phases of the Al-32.5 wt. % Cu- 1 wt. % Fe alloy were determined from FE-SEM and MAPPING images. α -Al, θ -Al₂Cu, ω -Al₇Cu₂Fe phases in Al-32.5 wt. % Cu- 1 wt. % Fe composition were determined. The composition of each phase was obtained by EDAX analysis.

Space group, crystal system and cell parameters were determined by XRD measurements of the alloy.

The magnetic properties of the alloy were determined. It was observed that alloy showed ferromagnetic properties from room temperature to the curie temperature, which is the magnetic transition temperature(T_c). When the magnetization M(H) curves were examined, it was seen that the magnetization decreased as the temperature increased.

Conflict interests

There are no conflicts of interest in this work.

References

- [1] Travessa D.N., Cardoso K.R., Wolf W., Jr. Jorge A.M., Botta W.J., The Formation of Quasicrystal Phase in Al-Cu-Fe System by Mechanical Alloying *Materials Research*, 15 (5) (2012) 749-752.
- [2] Školáková A., Novák P., Mejzliková L., Průša F., Salvetr P., Vojtěch D., Structure and Mechanical Properties of Al-Cu-Fe-X Alloys with Excellent Thermal Stability, *Materials (Basel) NOV*, 10 (11) (2017) 1269.

- [3] Huttunen-Saarivirta E., Microstructure, fabrication and properties of quasicrystalline Al–Cu–Fe alloys: A review., *J. Alloy. Compd.*, 363 (2004) 154–178.
- [4] Biswas K., and Chattopadhyay K., Formation of w-Al₇Cu₂Fe phase during laser processing of quasicrystal-forming Al–Cu–Fe alloy, *Philosophical Magazine Letters*, 88 3 (2008) 219-230.
- [5] Tsai A.P., Inoue A. and Masumoto T., A Stable Quasicrystal in Al–Cu–Fe System, *Jap. J. appl. Phys.*, 26 (9) (1987) L1505-L1507.
- [6] Liu W. and Köster U., Decomposition of the icosahedral phase in AlCuFe alloys, *Mater. Sci. Engng A*, 133 (1991) 388-392.
- [7] Gayle F.W., Shapiro A.J., Boancaniello F.S., et al., The Al–Cu–Fe phase diagram: 0 to 25 At. pct Fe and 50 to 75 At. Pct Al – Equilibria Involving the Icosahedral Phase, *Metall. Trans. A*, 23 (1992) 2409-2417.
- [8] Gratiyas D., Calvayrac Y., Devaud-Rzepski J., et al., Phase diagram and structures of the ternary AlCuFe system in the vicinity of the icosahedral region, *J. Non-Crystalline Solids* 153–154 (1993) 482-488.
- [9] Grushko B., Wittenberg R. and Holland-Moritz D., Solidification of Al–Cu–Fe alloys forming icosahedral phase, *J. Mater. Res*, 11 (1996) 2177-2185.
- [10] Gui J., Wang J., Wang R., et al., On some discrepancies in the literature about the formation of icosahedral quasicrystal in Al–Cu–Fe alloys, *J. Mater. Res*, 16 (2001) 1037-1046.
- [11] Rosas G. and Perez R., On the transformations of the ψ -AlCuFe icosahedral phase, *Mater. Lett*, 47 (2001) 225-230.
- [12] Zhang L. and Lück R., Z., Phase diagram of the Al–Cu–Fe quasicrystal-forming alloy system, *Metallkd*, 94 (2003) 91-97.
- [13] Auderbert F., Colaço R., Viller R., et al., Laser cladding of aluminium-base quasicrystalline alloys, *Scripta Mater*, 40 (1999) 551-557.
- [14] Biswas K., Galun R., Mordike B.L., et al., Laser cladding of quasicrystal forming Al–Cu–Fe on aluminum, *J. Non-Crystalline Solids*, 334–335 (2004) 517.
- [15] Zahoor A., Nawaz Shahid R., Tariq N.H., Wahab H., Anwar S., Rafiq M.A., Ameer A., Izhar S., Ali F., Hasan B.A., Effect on electrical and magnetic behavior of Al–Cu–Fe quasicrystals during surface leaching, *Applied Physics A*, (2021) 127, 551.
- [16] Yin S, Xie Z, Bian Q, He B, Pan Z, Sun Z et al., Formation of AlCuFe icosahedral quasicrystal by mechanical alloying: XAFS and XRD studies. *Journal of Alloys and Compounds*, 455 (1-2) (2008) 314-321.
- [17] Willey L.A., Metallography, Structures and Phase Diagrams, Vol.8, Metals Handbook 8th ed., American Society for Metals, Metals Park, OH. (1973)
- [18] Prevarskiy A.P., Investigation of Fe–Cu–Al Alloys, Russ. Metall. TR:Izv.Akad. Nauk SSSR, *Metall.*, 4 (1971) 154-156.
- [19] Yuan G.C., Influence of silicon content on friction and wear characteristics of new Al–Sn–Si alloys, *Chin. J. Nonferrous Metals*, 8 (9) (1998) 101-105.
- [20] Rudnev V., Loveless D., Cook R., Black M., Handbook of Induction Heating. Markel Dekker Inc, New York, (2003) 119-120.
- [21] Ari M., Saatçi B., Gündüz M., Payveren M., Durmus S., Thermo-electrical characterization of Sn–Zn alloys, *Mater. Char.*, 59 (2008) 757-763.
- [22] Zhou D.J., Study on Al–Sn–Si–Cu bearing alloy, *J. Light Alloy Fabr. Technol.*, 28 (5) (2000) 44-46.
- [23] Yamasue, E., Susa, M., Fukuyama, H., Nagata, K., Deviation from Wiedemann-Franz law for the thermal conductivity of liquid tin and lead at elevated temperature., *Int. J. Thermophys.* 24 (2003) 713-730.
- [24] Sergeant, E.J., Krum, A., Thermal management handbook: for electronic assemblies. 1 edition, McGraw-Hill Professional: New York, (1998) 26.
- [25] Bandyopadhyay, A. Dutta, Thermal, optical and dielectric properties of phase stabilized δ – Dy–Bi₂O₃ ionic conductors, *J. Phys. Chem. Solids*, 102 (2015) 12–20.
- [26] Büyük U., Maraşlı N., Çadırılı E., Kaya H., Keşlioğlu K., Variations of microhardness with solidification parameters and electrical resistivity with temperature for Al–Cu–Ag eutectic alloy., *Current Applied Physics* 12 (2012) 7-10.
- [27] Kaya H., Dependence of electrical resistivity on temperature and composition of Al–Cu alloys, *Materials Research Innovations*, 16 (3) (2012) 224-229.
- [28] Çadırılı E., Büyük U., Engin S., Kaya H., Effect of silicon on microstructure, mechanical and electrical properties of the directionally solidified Al-based quaternary alloys, *J. Alloys and Comp.*, 694 (2017) 471-479.
- [29] Youjun Z., Mingqiang H., Guangtao L., Chengwei Z., Vitali P.B., Eran G., Yingwei F., Jung-Fu L., Reconciliation of experiments and theory on transport properties of iron and the geodynamo. *Phys. Rev. Lett* 125 (2020) 0.78501.
- [30] Touloukian Y.S., Powell R.W., Ho C.Y., Klemens P.G., Thermal Conductivity Metallic Elements and Alloys, vol. 1, New York, Washington, (1970) 60.
- [31] Choi S.W., Cho H.S., Kumai S., Effect of the precipitation of secondary phases on the thermal diffusivity and thermal conductivity of Al–4.5 Cu alloy, *J. Alloys and Comp.* 688 (2016) 897-902.
- [32] Nguyen H. V., Do N. B., Nguyen T. H. O., Nguyen C. S., Trinh V. T., Le H. T., Junior A. M. J., Synthesis and magnetic properties of Al–Cu–Fe quasicrystals prepared by mechanical alloying and heat treatment, *J. of Materials Research*, 38 (2023) 3 644-653.
- [33] Oanha N. T. H., Vieta N. H., Dudina D. V., Jorge Jr A. M., Kimi Ji-Soon, Structural characterization and magnetic properties of Al₈₂Fe₁₆TM₂ (TM: Ti, Ni, Cu) alloys prepared by mechanical alloying, *J. of Non-Crystalline Solids*, 468 (2017) 67-73.
- [34] Li Z., Bai H. Y., Pan M. X., Zhao De Q., Wang W. L., Wang W. H., Formation, properties, thermal characteristics, and crystallization of hard magnetic Pr–Al–Fe–Cu bulk metallic glasses, *J. Mater. Res.*, Vol. 18 (2003) 9 2208-2213.